

# Temporal Landmark Validation in CML

Juan Andrade-Cetto and Alberto Sanfeliu  
Institut de Robòtica i Informàtica Industrial, UPC-CSIC  
Llorens Artigas 4-6, 08028 Barcelona, Spain  
{chetto,sanfeliu}@iri.upc.es

**Abstract**— Current techniques to concurrent map building and localization (CML) have been devised for static environments, and lack robustness in more realistic situations. In this communication we provide new ideas that extend the typical stochastic estimation approach to CML, to take into account the dynamics of the environment. The basic idea consists on using the history of data association mismatches for the computation of the likelihood of future data association. The incorporation of a novel temporal landmark quality test, together with the spatial compatibility tests already available, help alleviate the difficulty of data association.

We propose a pair of temporal landmark quality functions to aid in those situations in which landmark observations might not be consistent in time; and show how by incorporating these functions, the overall estimation-theoretic approach to CML is improved. Special attention is paid in that the removal of landmarks from the map does not violate the basic convergence properties of the localization and map building algorithms already described in the literature. Namely, asymptotic convergence and full correlation.

## I. INTRODUCTION

The use of stochastic models for map building and localization in mobile robotics has gained much popularity in recent years. Of particular interest is the use of predictive filters to estimate the robot position and uncertainty, and to update these estimates from sensor readings while at the same time building an incremental map of the environment [1]–[4].

One of the most critical limitations in the application of such estimation-theoretic approaches to map building and localization is the data association problem. Data association refers to the issue of matching observations with previously learned elements from the environment. As we address issues such as viewpoint invariance and feature extraction from sensor data, it is overwhelming how undesired environment dynamics, occlusions, and sensor noise can still make data association a daunting task. One possibility to overcome the data association problem altogether is with the deployment of uniquely identifiable man-made beacons to aid in localization. Unfortunately, there exist multiple situations where this is not possible, and a map must still be constructed without environment contamination. An alternative approach explored in this work is the inclusion of temporal landmark quality measures, along with the already available spatial compatibility tests.

We start our discussion with a short review of the traditional full covariance extended Kalman filter approach to concurrent map building and localization (EKF-CML in short). Next, we present the two temporal landmark quality measures proposed that help alleviate the data association problem. We then show that when testing for temporal landmark compatibility with

these functions it is still possible to achieve a monotonically decreasing map covariance matrix, and how in the limit, the map still becomes fully correlated. That is, the two fundamental properties of the EKF-CML algorithm first reported in Newman's PhD work [5] hold also in our revised version, the EKF-CML-LV algorithm.

In Section IV, explicit formulas for a planar mobile robot are presented. Finally, in Section V, our planar mobile robot configuration is used to evaluate the original EKF-CML algorithm as reported by Smith and Cheeseman [4], as well as our improved algorithm, the EKF-CML-LV, both in the presence of various noise levels, and ultimately, in cases with limited field of view and extreme data mismatch.

## II. FULL COVARIANCE APPROACH TO CML

In the typical EKF-CML model, the state vector  $\mathbf{x}_k$  includes the position of the robot  $\mathbf{x}_{r,k}$  at time step  $k$ , and a vector of stationary map features  $\mathbf{x}_f$ . The input vector  $\mathbf{u}_k$  indicates the vehicle control command, and  $\mathbf{v}_k$  is a random vector with zero mean and covariance matrix  $\mathbf{V}_k$ , representing unmodelled robot dynamics and system noise. A possibly nonlinear difference equation  $\mathbf{f}(\mathbf{x}_k, \mathbf{u}_k, \mathbf{v}_k)$  is used to model the motion of the robot. Furthermore, the random vector  $\mathbf{w}_k$  represents both, the inaccuracies of the also possibly nonlinear observation model  $\mathbf{h}(\mathbf{x}_k, \mathbf{w}_k)$ , and the measurement noise with zero mean and covariance matrix  $\mathbf{W}_k$ .

### A. Prediction

An a priori prediction of the location of the robot and the state of the map is obtained from the noise free state dynamics

$$\begin{bmatrix} \mathbf{x}_{r,k+1|k} \\ \mathbf{x}_{f,k+1|k} \end{bmatrix} = \begin{bmatrix} \mathbf{f}_{r,k}(\mathbf{x}_{r,k|k}, \mathbf{u}_k, \mathbf{0}) \\ \mathbf{x}_{f,k|k} \end{bmatrix} \quad (1)$$

and the a priori estimate to the map state error covariance is  $\mathbf{P}_{k+1|k} = \mathbf{F}_x \mathbf{P}_{k|k} \mathbf{F}_x^T + \mathbf{F}_v \mathbf{V}_k \mathbf{F}_v^T$ . The Jacobian matrices  $\mathbf{F}_x$  and  $\mathbf{F}_v$  contain the partial derivatives of  $\mathbf{f}$  with respect to  $\mathbf{x}$  and  $\mathbf{v}$ . Similarly, noise free sensor measurements can be estimated a priori with  $\mathbf{z}_{k+1|k} = \mathbf{h}(\mathbf{x}_{k+1|k}, \mathbf{0})$ .

### B. Correction

The vehicle and map state estimates are revised in an EKF fashion from the difference between estimated and actual sensor measurements

$$\tilde{\mathbf{z}}_{k+1|k} = \mathbf{z}_{k+1} - \mathbf{z}_{k+1|k} \quad (2)$$

$$\mathbf{x}_{k+1|k+1} = \mathbf{x}_{k+1|k} + \mathbf{K}_{k+1} \tilde{\mathbf{z}}_{k+1|k} \quad (3)$$

and the error covariance matrix updated with the Joseph form

$$\mathbf{P}_{k+1|k+1} = (\mathbf{I} - \mathbf{K}_{k+1}\mathbf{H}_x)\mathbf{P}_{k+1|k}(\mathbf{I} - \mathbf{K}_{k+1}\mathbf{H}_x)^\top + \mathbf{K}_{k+1}\mathbf{W}_{k+1}\mathbf{K}_{k+1}^\top \quad (4)$$

with  $\mathbf{K}_{k+1} = \mathbf{P}_{k+1|k}\mathbf{H}_x^\top\mathbf{S}^{-1}$  the Kalman matrix gain,  $\mathbf{S}$  the measurement innovation matrix (see Eq. 10), and  $\mathbf{H}_x = [\mathbf{H}_{x_r} \quad \mathbf{H}_{x_f}]$  the measurement Jacobian, i.e., the derivative of  $\mathbf{h}$  with respect to  $\mathbf{x}$ .

### C. Sequential innovation

Sequential innovation refers to the update of state estimates one observation at a time. The result of applying this technique is equivalent to that of using the full covariance extended Kalman filter approach, provided the observations are independent, or that at least they can be whitened.

The main advantage of using sequential innovation is that, by considering the measurement innovation vector  $\mathbf{z}_{k+1}$  as a set of single measurements  $\mathbf{z}_{k+1}^{(i)}$  that can be treated sequentially, the measurement of the joint measurement innovation covariance matrix  $\mathbf{S}$  in equation 4 is no longer necessary. Instead, a series of smaller individual innovation covariance matrix inverses is computed, reducing considerably the time complexity of the algorithm.

### D. Covariance initialization

The function that maps an observation into world coordinates is given by our linearized measurement model, and has the form  $[\mathbf{x}_r^\top, \mathbf{x}_f^{(i)\top}]^\top = \mathbf{G}[\mathbf{x}_r^\top, \mathbf{z}^{(i)\top}]^\top$ .  $\mathbf{G}$  is known as the *feature initialization matrix*,

$$\mathbf{G} = \begin{bmatrix} \mathbf{I} & \mathbf{0} \\ -\mathbf{H}_{x_f}^{-1}\mathbf{H}_{x_r} & \mathbf{H}_{x_f}^{-1} \end{bmatrix} \quad (5)$$

The initialization of the corresponding map state error covariance for such landmark is given by

$$\mathbf{P} = \mathbf{G} \begin{bmatrix} \mathbf{P}_{rr} & \mathbf{0} \\ \mathbf{0} & \mathbf{W}^{(i)} \end{bmatrix} \mathbf{G}^\top \quad (6)$$

Once the robot has observed a sufficiently robust new feature which cannot be associated to any other landmark in the map, it is labeled as the  $n$ -th landmark, and a new row and column must be appended to the map covariance matrix with

$$\mathbf{P}_{rf^{(n)},k|k} = -\mathbf{P}_{rr,k|k}(\mathbf{H}_{x_f}^{-1}\mathbf{H}_{x_r^{(n)}})^\top \quad (7)$$

$$\mathbf{P}_{f^{(i)}f^{(n)},k|k} = \mathbf{H}_{x_f}^{-1}\mathbf{H}_{x_r^{(i)}}\mathbf{P}_{rr,k|k}(\mathbf{H}_{x_f}^{-1}\mathbf{H}_{x_r^{(n)}})^\top \quad (8)$$

$$\mathbf{P}_{f^{(n)}f^{(n)},k|k} = \mathbf{H}_{x_f}^{-1}\mathbf{H}_{x_r^{(n)}}\mathbf{P}_{rr,k|k}(\mathbf{H}_{x_f}^{-1}\mathbf{H}_{x_r^{(n)}})^\top + \mathbf{H}_{x_f}^{-1}\mathbf{W}^{(i)}(\mathbf{H}_{x_f}^{-1})^\top \quad (9)$$

Eqs. 7-9 indicate that the initialization of the new feature map error covariance is a function of the actual vehicle position and its accumulated uncertainty.

### E. Spatial compatibility

The estimated uncertainty in the localization of every landmark in the map, as well as that of the robot, is maintained in the state error covariance  $\mathbf{P}$ . The uncertainty of its location in observation space is given by the change of basis of  $\mathbf{P}$  plus that of the independent sensor uncertainties  $\mathbf{W}^{(i)}$ . This quantity is called the innovation covariance matrix, and is given by the expression

$$\mathbf{S}^{(i)} = \mathbf{H}_x^{(i)}\mathbf{P}_{k+1|k}\mathbf{H}_x^{(i)\top} + \mathbf{H}_w^{(i)}\mathbf{W}_{k+1}^{(i)}\mathbf{H}_w^{(i)\top} \quad (10)$$

For any particular landmark measurement  $\mathbf{z}_{k+1}^{(i)}$ , the squared Mahalanobis distance

$$d_i^2 = \mathbf{z}_{k+1|k}^{(i)\top} \mathbf{S}^{(i)-1} \mathbf{z}_{k+1|k}^{(i)} \quad (11)$$

represents a measure of spatial disparity between the observation  $\mathbf{z}_{k+1}^{(i)}$  and the estimated location in robot centered coordinates of the hypothetical landmark match  $\mathbf{x}_f^{(i)}$ .

Two spatial landmark compatibility tests that appear in the literature are the individual compatibility test:

$$d_i^2 \leq \chi_{\dim \mathbf{z}^{(i)}, \alpha}^2 \quad (12)$$

and the joint compatibility test [6]:

$$d_{p\dots r}^2 = \mathbf{z}_{k+1|k}^{(p\dots r)\top} \mathbf{S}^{(p\dots r)-1} \mathbf{z}_{k+1|k}^{(p\dots r)} \quad (13)$$

$$d_{p\dots r}^2 \leq \chi_{\dim \mathbf{z}^{(p\dots r)}, \alpha}^2 \quad (14)$$

the indices  $(p\dots r)$  need not be consecutive. The former considers landmark observations independently; whereas the latter, considers cross correlated landmark uncertainties when testing match hypotheses, at the expense of higher computational cost.

### F. Convergence properties of the full covariance EKF approach to CML

It has been shown [2] how in the original full covariance EKF-CML formulation, the map state error covariance submatrix associated with the landmark estimates decreases monotonically as successive observations take place, and how in the limit, as the number of iterations tends to infinity, the map becomes fully correlated.

$$\det \mathbf{P}_{ff,k+1|k+1} \leq \det \mathbf{P}_{ff,k|k} \quad (15)$$

$$\lim_{k \rightarrow \infty} \det \mathbf{P}_{ff,k|k} = 0 \quad (16)$$

We show later in this contribution how the removal of temporally weak landmark does not violate these two properties.

## III. LANDMARK TEMPORAL UNCERTAINTY

Spatial compatibility tests are crucial for the solution of data association in CML, but they can still be insufficient in situations with moderate scene dynamics. Consider for example the case when a landmark is occluded for a short period of time. The spatial compatibility tests would not have any information on the history of observations of such landmark, and might still be trying to wrongly associate it with a neighboring observed feature. If the algorithm succeeds in incorrectly associating the occluded feature, it will enlarge the uncertainty of that

landmark in the map; and given that the map covariance is fully correlated, starting with the next iteration of the algorithm, that uncertainty would be propagated to the rest of the landmark locations, and that of the robot as well; ultimately breaking down the entire estimation approach to CML.

To aid in those situations in which the landmark observations might not be consistent in time, we propose a new set of landmark quality functions, that take into account the history of data association mismatches.

#### A. Nonlinear model for temporal landmark quality: the exponential decay rule

One possibility in the computation of the temporal landmark quality is to have an exponential decay rule [7]. This way, each landmark in the map will have an associated memory cell that registers how persistent, and how old that landmark is.

Imagine that at the  $k + 1$ -th iteration, the  $i$ -th landmark measurement estimate  $\mathbf{z}_{k+1|k}^{(i)}$  falls inside the current field of view, but none of the entries in the observation vector  $\mathbf{z}_{k+1}$  has similar appearance properties, nor is sufficiently close (in the sense of  $d^2$ ) to pass the spatial landmark compatibility tests. This would be the situation if, for example, the  $i$ -th landmark was learned from a temporary artifact in the scene that was only tracked over sensor data for a short period of time, but is no longer present. With the aid of an exponential decay rule to data association, its quality measure will decay in the absence of observation matches, indicating the map building algorithm that such landmark is no longer present in the scene and should not be considered a relevant feature for robot localization.

We propose a nonlinear update rule for landmark quality of the form

$$x_{q,k+1}^{(i)} = \frac{1}{1 + e^{-(\alpha u_{q,k}^{(i)} + \beta x_{q,k}^{(i)})}} \quad (17)$$

where  $u_{q,k}^{(i)}$  is the landmark identification stamp

$$u_{q,k}^{(i)} = \begin{cases} 0 & : \text{ failed the spatial data association test} \\ 1 & : \text{ passed the spatial data association test} \end{cases} \quad (18)$$

The scalar  $\alpha$  is an input weight used to regulate the contribution of such landmark identification over the previous map configuration, and  $\beta$  is a memory weight used to regulate the contribution of the previous landmark quality state over its new value.

The asymptotic lower and upper bounds of Eq. 17 can be evaluated by solving the equations

$$x_{q,LOW} = \frac{1}{1 + e^{-(\beta x_{q,LOW})}} \quad (19)$$

$$x_{q,HIGH} = \frac{1}{1 + e^{-(\alpha + \beta x_{q,HIGH})}} \quad (20)$$

Using a symbolic manipulation math package, we find for example, that for  $\alpha = \beta = 1$ ,  $x_{q,LOW} = 0.6590$ , and  $x_{q,HIGH} = 0.8659$ . Landmark initialization is at the middle of the scale, i.e.  $x_{q,0}^{(i)} = 0.7682$ .

#### B. Linear model for temporal landmark quality: the data association probability

Another possibility in the computation of the temporal landmark quality is to consider the probability of correct data association of such landmark in the next iteration.

According to the relative frequency definition of probability, if an event (say, the correct association of landmark  $i$ ) occurs  $j$  times in  $k$  trials (observations), and provided  $k$  is sufficiently large, then the probability that the same landmark will be properly matched in the next iteration can be expressed as  $p_k^{(i)} = j/k$ .

Now, once a new observation is made, the data association probability will change according to the new landmark association result. This change in probability is represented by the recursivity  $p_{k+1}^{(i)} = (p_k^{(i)}k + u_{q,k}^{(i)})/(k+1)$ , with  $u_{q,k}^{(i)}$  defined as in Eq. 18. If we make the notation change  $a = k/(k+1)$ , and  $x_{q,k}^{(i)} = p_k^{(i)}$ , our second model for temporal landmark quality becomes

$$x_{q,k+1}^{(i)} = ax_{q,k+1}^{(i)} + (1-a)u_{q,k}^{(i)} \quad (21)$$

For fixed values of  $k$ , the constant  $a$  accounts for a memory weight with a role similar as those of  $\alpha$  and  $\beta$  from the previously discussed model. It can be fixed to a constant value between 0 and 1, and it indicates the memory length to be used in the computation of the new data association probability. So for example, if a memory window of the last 5 iterations is to be considered, the memory weight becomes  $a = 0.8333$ . In this linear model for temporal landmark quality,  $x_q$  is bounded between 0 and 1, and initialization is made at 0.5.

Both temporal landmark quality measures, the exponential decay rule, and the data association probability were chosen to be asymptotically bounded by above and below by

$$x_{q,LOW} \leq x_q \leq x_{q,HIGH} \quad (22)$$

Any other function with such monotonicity could be also used as temporal landmark quality function. However, such function must have some way of tuning the memory length of the algorithm. The left plot in Fig. 1 shows the behavior of the exponential decay rule for the parameter values  $\alpha = \beta = 1$ . The right plot shows the data association probability with parameter  $a = 0.5$ . The labels 0-1 and 1-0 indicate the change in the landmark identification stamp  $u_q$ , representing the presence or loss of data association.

#### C. Temporal landmark quality test

In the same way that the spatial compatibility test is used to validate if observations are consistent with the already learned map entries; the temporal landmark quality test must be used to validate if any map entry is sufficiently robust to be kept in the map. The test verifies if the history of data association has kept the value for the temporal landmark quality above a user defined cut threshold  $x_{q,THLD}$ . All landmarks expected to appear in the current field of view, and for which no occlusion has been predicted, must have their landmark quality measure updated. Furthermore, those landmarks whose temporal quality measure falls below the user defined threshold should be removed from the map. The

heuristics needed to handle occlusions, depend on the type of landmarks and sensors used. The temporal landmark quality test is

$$\text{if } x_q^{(i)} \leq x_{q,THLD} \quad (23)$$

$$\text{RemoveLandmark}(x_f^{(i)})$$

In the case of the exponential decay rule with parameters  $\alpha = \beta = 1$ , for example, the cut threshold  $x_{q,THLD} = 0.66$  is reached once a landmark has not been observed for 5 consecutive iterations, or more if these were not consecutive. Similar effects are obtained when using the data association probability with the parameter value  $a = 0.5$ , and a cut threshold of  $x_{q,THLD} = 0.03$ . Fig. 2 shows both the exponential decay rule, and the data association probability as landmark quality measures for a test run of 100 steps and 10 landmarks, when 25% of the observations are misidentified to their closest neighbor. The individual compatibility test catches some but not all of these mismatches, and yields an identification stamp value  $u_q = 0$  for them. By adding the more restrictive temporal landmark quality tests, those landmarks with a large amount of mismatches end up being removed from the map, and are reinitialized as new landmarks once they become robust again.

We have opted for a simplified heuristic for the removal of a landmark from the map, with the advantage of computational efficiency, but at the expense of suboptimality. Our algorithm simply erases the low quality landmark entries from the state vector and its corresponding row and column in the state error covariance matrix. Once the landmark is robust again, it is considered as a new different landmark, and initialized according to the discussion from Section II-D. Note however that, given the fact that CML is fully correlated, the contribution of a misidentified landmark estimate in revising the error covariance matrix has already propagated to the entire map. The right thing to do, would be to trace back the intermediate results of the algorithm up to the point in which the landmark was originally inserted, and to recompute forward once more the map state and map error covariance up to the current iteration, without considering that landmark, as if it had never existed.

Saving the state vector and error covariance matrix for all iterations has space complexity of  $O(kn^2)$ , with  $k$  the number of iterations, and  $n$  the number of landmarks. Furthermore, recomputing the state vector and error covariance matrix from the point at which the spurious landmark was initially inserted, would most likely lead to different values on  $\mathbf{P}$ , and consequently on  $\mathbf{S}$ , producing even different data association results. So, not only the state vector and covariance matrix history must be maintained, but the full measurement data as well, requiring for a full run of the algorithm every time a landmark is found to be spurious. The optimal solution is rather cumbersome, and we have opted for suboptimality, with the aforementioned simplification of just deleting the corresponding entries in  $\mathbf{x}$  and  $\mathbf{P}$ , with the following insight.

Gibbens *et al.* [8], show how in CML all entries in the covariance matrix  $\mathbf{P}$  depend on the number of landmarks

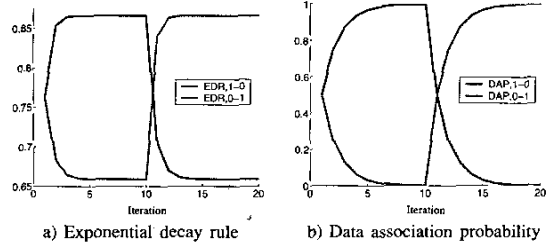


Fig. 1. Landmark quality models.

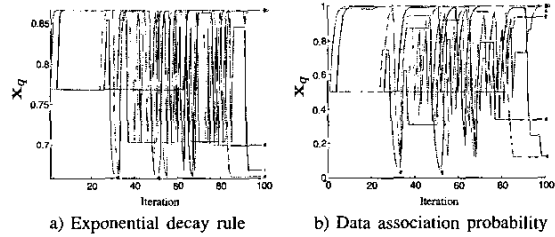


Fig. 2. Landmark quality test for a test run with 10 landmarks and 100 steps.  $\alpha = \beta = 1$ , and  $a = 0.5$ .

used in the form of the total Fisher information  $I_T$ . This is a measure of the total information per unit time available to the filter. For a monobot (monodimensional robot) with  $n$  landmarks, all with equal measurement covariance  $\mathbf{W}^{(i)} = w$ , the total Fisher information is  $I_T = n/w$ . The more landmarks available, the more information the filter has. That is, the greater the number of landmarks used, the smaller the asymptotic values for the entries in the error covariances.

The removal of a landmark from the state vector in the form discussed is consistent with this observation. Fig. 3a shows, how for the monobot, all the entries in  $\mathbf{P}$  with the removal of a landmark at some point in the algorithm are bounded by below and above by the same entries in  $\mathbf{P}$ , but with and without considering the landmark for the entire run. Let us call  $\mathbf{P}_{\cdot, n}$  the entry in  $\mathbf{P}$  for a map with  $n$  landmarks, and  $\mathbf{P}_{\cdot, n+1, n}$  the entry in  $\mathbf{P}$  for a map that went from  $n+1$  to  $n$  landmarks via the removal of landmark states. Then, for the entire run of the algorithm

$$\mathbf{P}_{rr, k|k, n+1} \leq \mathbf{P}_{rr, k|k, n+1, n} \leq \mathbf{P}_{rr, k|k, n} \quad (24)$$

$$\mathbf{P}_{rf, k|k, n+1}^{(i)} \leq \mathbf{P}_{rf, k|k, n+1, n}^{(i)} \leq \mathbf{P}_{rf, k|k, n}^{(i)} \quad (25)$$

$$\mathbf{P}_{ff, k|k, n+1}^{(i, j)} \leq \mathbf{P}_{ff, k|k, n+1, n}^{(i, j)} \leq \mathbf{P}_{ff, k|k, n}^{(i, j)} \quad (26)$$

Moreover, by removing a landmark from the map in the form discussed, the asymptotic convergence property from Eq. 16 is maintained. That is, the revised map is still fully correlated, as indicated in Fig. 3b.

#### IV. PLANAR MOBILE ROBOT

For the mobile robot shown in Fig. 6, the vehicle state is defined by  $\mathbf{x}_r = [x, y, \theta]^T$  where  $x$  and  $y$  are the center of the robot with respect to some global coordinate frame, and  $\theta$  is the vehicle orientation. The vehicle control command  $\mathbf{u}_r = [u_x, u_y, u_\theta]^T$  indicates the desired positional increments

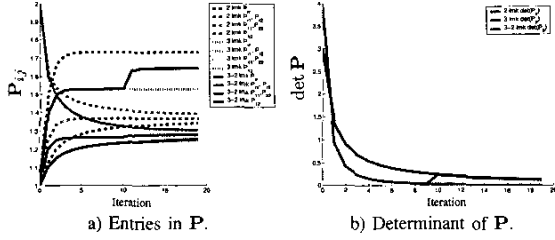


Fig. 3. Evolution of the covariance matrix for a monobot with 3, 2, and 3-then-2 landmarks.  $\mathbf{V} = \mathbf{W}^{(i)} = \mathbf{P}_{rr,0|0} = \mathbf{I}$ .

to the vehicle pose in robot local coordinates; with vehicle error dynamics  $\mathbf{v}_r = [v_x, v_y, v_\theta]^T$ . We can observe how for an error free vehicle, the input  $(u_{x,k}, u_{y,k})$  would drive the robot to the position  $(x_{k+1|k}, y_{k+1|k})$  at time step  $k$ . However, due to unmodelled robot dynamics and noise, it ends up in the position  $(x_{k+1}, y_{k+1})$ . This is, the vehicle process model  $\mathbf{f}_r$  is a noise-corrupted discrete-time nonlinear function of the form

$$\begin{bmatrix} x_{k+1} \\ y_{k+1} \\ \theta_{k+1} \end{bmatrix} = \begin{bmatrix} x_k + d_u \cos(\theta_k + \psi_u) + d_v \cos(\theta_k + \psi_v) \\ y_k + d_u \sin(\theta_k + \psi_u) + d_v \sin(\theta_k + \psi_v) \\ \theta_k + u_{\theta,k} + v_{\theta,k} \end{bmatrix} \quad (27)$$

with  $d_u = \sqrt{u_{x,k}^2 + u_{y,k}^2}$ ,  $d_v = \sqrt{v_{x,k}^2 + v_{y,k}^2}$ ,  $\psi_u = \arctan(u_{y,k}/u_{x,k})$ , and  $\psi_v = \arctan(v_{y,k}/v_{x,k})$ .

Given that the map is considered static  $\mathbf{f}_f(\mathbf{x}_k, \mathbf{u}_k, \mathbf{v}_k) = \mathbf{x}_f$ , and that the landmarks are constituted by two dimensional points  $\mathbf{x}_f^{(i)} = [x_f^{(i)}, y_f^{(i)}]^T$ ; we are able to formulate the partial derivatives of Eq. 27 with respect to  $\mathbf{x}$  and  $\mathbf{v}$  for the state model Jacobians

$$\mathbf{F}_{\mathbf{x}_r} = \begin{bmatrix} 1 & 0 & -d_u \sin(\theta_k + \psi_u) - d_v \sin(\theta_k + \psi_v) \\ 0 & 1 & d_u \cos(\theta_k + \psi_u) + d_v \cos(\theta_k + \psi_v) \\ 0 & 0 & 1 \end{bmatrix}$$

$$\mathbf{F}_{\mathbf{v}_r} = \begin{bmatrix} v_{x,k} \cos(\theta_k + \psi_u)/d_u & v_{y,k} \cos(\theta_k + \psi_u)/d_u & 0 \\ v_{x,k} \sin(\theta_k + \psi_u)/d_u & v_{y,k} \sin(\theta_k + \psi_u)/d_u & 0 \\ 0 & 0 & 1 \end{bmatrix}$$

The measurement equation for the  $i$ -th landmark in this configuration is  $\mathbf{h}^{(i)} = \mathbf{R}^T(\mathbf{x}_f^{(i)} - \mathbf{t}) + \mathbf{w}^{(i)}$ , with  $\mathbf{w}^{(i)}$  the landmark observation error, and

$$\mathbf{R} = \begin{bmatrix} \cos(\theta_k) & -\sin(\theta_k) \\ \sin(\theta_k) & \cos(\theta_k) \end{bmatrix}, \quad \mathbf{t} = \begin{bmatrix} x_k \\ y_k \end{bmatrix} \quad (28)$$

The  $i$ -th set of rows of the measurement and noise Jacobians for our planar mobile robot are  $\mathbf{H}_{\mathbf{x}}^{(i)} = [-\mathbf{R}^T, \mathbf{R}^T(\mathbf{x}_f^{(i)} - \mathbf{t}), \mathbf{0}_{2 \times 2(i-1)}, \mathbf{R}^T, \mathbf{0}_{2 \times 2(N-i)}]$ , and  $\mathbf{H}_{\mathbf{w}}^{(i)} = \mathbf{I}$ .

## V. PERFORMANCE OF THE CML-LV ALGORITHM

We present now results on the improvement in the reconstruction achieved with the various modifications to the EKF-CML model proposed in this work. We will concentrate on the situation of erroneous data association, which is considered one of the most critical artifacts that might destroy the viability of the EKF-based method to concurrent localization and map building.

From this point on we will consider as our standard test case, and unless otherwise indicated, a planar robot with 3 dof traversing an environment with 10 landmarks in 100 steps.

### A. Data mismatch

Consider the situation where the landmark identification module is not error-free. Such is the case when we allow the system a percentage of landmark identification mismatches. Imagine that we observe say visual landmarks, such as corners or lines extracted from intensity images, and that our landmark tracking algorithm is not very accurate at matching observations in consecutive frames upon illumination changes. For the sample run shown in Fig. 4a, landmark matching is performed with a 25 percent probability of mismatch within a  $1m$  radius, and with a sensor with a limited field of view of  $2m$ .

Localization and map building proceeds smoothly until the first mismatch occurs. The algorithm is not able to recover from this failure, and when the previously observed landmarks re-enter the field of view two things happen. On the one hand, the new observations of the already learned landmarks aid in reversing the error trend in localization; and on the other hand, the same new observations are used to revise the other location estimates of those landmarks. The contribution to the revision of the robot pose and landmark location estimates will be proportional to our degree of trust in the motion and sensor models respectively. If the plant error covariance  $\mathbf{V}$  is large, and the measurement error covariance  $\mathbf{W}$  is small, the EKF-CML algorithm trusts more on the observations than on dead-reckoning, revising more heavily the robot pose estimate than that of the landmarks. Conversely, when the measurement error covariance is larger than the plant error covariance, the algorithm trusts more on the motion of the robot and ends up revising more heavily the landmark estimates.

Even when the effects of using a limited field of view can lead to inaccurate localization estimates, we have seen that the effects of data mismatch are the most pervasive artifact in CML. Given the fact that the map is fully correlated, landmark mismatch effects propagate to the localization estimate of all the landmarks in the model.

The estimation theoretic approach to CML, as presented by Smith and Cheeseman, and later refined by Leonard, Newman, Durrant-Whyte, Neira, and Tardós among others, is very sensitive to data association errors; and as formulated lacks a theoretical foundation to deal with the problem. Efforts have been tailored at correcting the effects of data mismatches, and at finding measures of the spatial compatibility of landmark correspondence. We go one step further, providing a new formulation in which temporal landmark quality measures are also present.

### B. Landmark validation

We present now results of the two strategies for the computation of landmark quality herein discussed. First, we show the results of using the compatibility test to validate landmark observations in terms of their location within the measurement innovation covariance only, as discussed in [6]. Fig. 4b shows the improvement in the localization of the mobile robot when the spatial compatibility test from Eq. 12 ( $\chi^2$  goodness of fit test) is performed, with a confidence level of 95%.

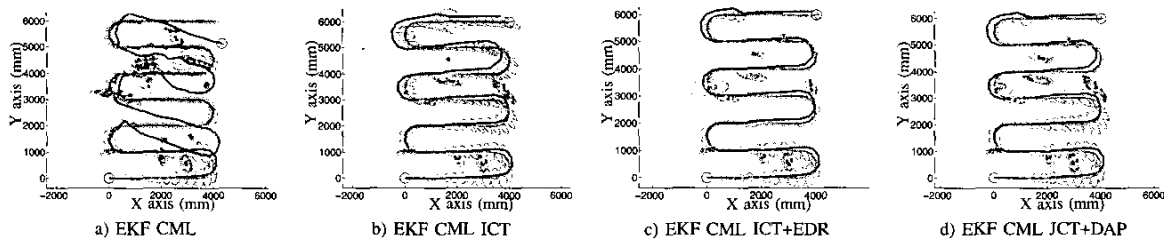


Fig. 4. Full-covariance EKF CML for a path with 100 iterations and 10 landmarks, and a sensor with a limited radius of observation of 2m. Data mismatch occurs within a radius of 1m with a 25% probability.

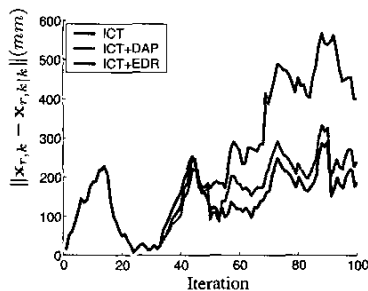


Fig. 5. Robot localization error estimate.

Next, we include the temporal landmark quality test to our results. Those landmarks whose probability of association falls below a given threshold are reinitialized in the map. This is, they can no longer be used for localization. Figs. 4c and d show the improvement of using the two temporal landmark quality tests together with spatial landmark quality association in CML.

Lastly, we plot in Fig. 5 the norm of the robot localization error in the  $xy$  plane to show a comparison between the original EKF-CML algorithm with limited vision range and data association errors (realistic case of CML); the advantage of using the individual compatibility test; and the improvements proposed using both the spatial and temporal compatibility tests: DAP the data association probability, and EDR: the exponential decay rule. Fig. 6 shows a sample application of EKF-CML-LV over a real environment.

## VI. CONCLUSIONS

This article presents a revision of the traditional full-correlation EKF CML algorithm for mobile robot localization and map building. We extend the traditional algorithm by adding temporal landmark quality measures, and a temporal landmark quality test to validate the history of data association. These quality measures permit the maintenance of the map by the elimination of inconsistent observations. The removal of weak landmarks from the state vector and state covariance matrix does not violate the convergence properties of CML. Special attention has been paid in the selection of the temporal landmark quality models, to guarantee that the uncertainty in

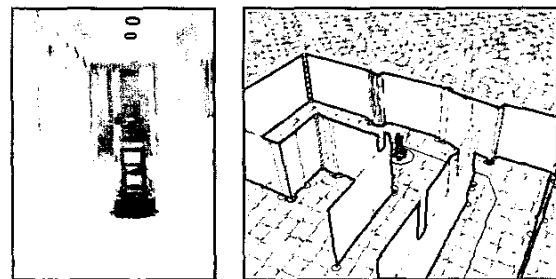


Fig. 6. EKF-CML-LV on a real environment.

the map estimates still reduces monotonically. The proposed solution contributes in simplifying the data association problem in CML.

## ACKNOWLEDGEMENTS

This work was partially supported by the Spanish Council of Science and Technology under project DPI 2001-2223.

## REFERENCES

- [1] J. A. Castellanos, J. M. M. Montiel, J. Neira, and J. D. Tardós, "The SPMAP: A probabilistic framework for simultaneous localization and map building," *IEEE Trans. Robot. Automat.*, vol. 15, no. 5, pp. 948–952, Oct. 1999.
- [2] M. W. M. G. Dissanayake, P. Newman, S. Clark, H. F. Durrant-Whyte, and M. Csorba, "A solution to the simultaneous localization and map building (SLAM) problem," *IEEE Trans. Robot. Automat.*, vol. 17, no. 3, pp. 229–241, Jun. 2001.
- [3] J. J. Leonard, H. F. Durrant-Whyte, and I. J. Cox, "Dynamic map building for an autonomous mobile robot," *Int. J. Robot. Res.*, vol. 11, no. 4, pp. 286–292, 1992.
- [4] R. C. Smith and P. Cheeseman, "On the representation and estimation of spatial uncertainty," *Int. J. Robot. Res.*, vol. 5, no. 4, pp. 56–68, 1986.
- [5] P. M. Newman, "On the structure and solution of the simultaneous localization and map building problem," Ph.D. dissertation, The University of Sydney, Sydney, Mar. 1999.
- [6] J. Neira and J. D. Tardós, "Data association in stochastic mapping using the joint compatibility test," *IEEE Trans. Robot. Automat.*, vol. 17, no. 6, pp. 890–897, Dec. 2001.
- [7] J. Andrade-Cetto and A. Sanfeliu, "Learning of dynamic environments by a mobile robot from stereo cues," in *Proc. IEEE Int. Conf. Multisensor Fusion Integration Intell. Syst.*, Baden-Baden, Aug. 2001, pp. 305–310.
- [8] P. W. Gibbens, G. M. W. M. Dissanayake, and H. F. Durrant-Whyte, "A closed form solution to the single degree of freedom simultaneous localization and map building (SLAM) problem," in *Proc. IEEE Int. Conf. Decision Control*, Sydney, Dec. 2000, pp. 408–415.